Click Here for Full Article

Diurnal variation and radiative influence of Martian water ice clouds

R. John Wilson,[1] Gregory A. Neumann,[2] and Michael D. Smith[2]

[1]   We have identified regions in the Martian tropics with anomalously warm nighttime surface temperatures. The seasonal evolution of these anomalies is strongly correlated with the waxing and waning of the tropical cloud belt that is most prominent during Northern Hemisphere summer. We attribute the anomalies to enhanced downward infrared radiation from water ice clouds. The close agreement with spatial maps of atmospheric extinction derived from Mars Orbiter Laser Altimeter radiometry strongly supports this interpretation. We show that a Mars general circulation model simulation with radiatively active water ice clouds is able to reasonably match the observed spatial pattern and amplitude of the surface temperature anomaly. The nighttime clouds are most prominent in the Tharsis and Arabia regions and are thicker (optical depth ~ 1) and more extensive than daytime clouds. Our cloud retrievals are the first to spatially map the nighttime clouds and provide an estimate of their thermal influence. **Citation:** Wilson, R. J., G. A. Neumann, and M. D. Smith (2007), Diurnal variation and radiative influence of Martian water ice clouds, *Geophys. Res. Lett.*, *34*, L02710, doi:10.1029/2006GL027976.

1. Introduction

[2]   The aphelion season is characterized by the presence of a prominent tropical water ice cloud belt [*Clancy et al.*, 1996; *Smith*, 2004]. Recent Mars general circulation model (MGCM) simulations have indicated that water ice clouds play an important role in the Martian water cycle [*Richardson et al.*, 2002; *Montmessin et al.*, 2004; *Feldman et al.*, 2005]. Simulations suggest that the tropical cloud belt undergoes a significant diurnal cycle, with maximum opacity in the early morning hours [*Hinson and Wilson*, 2004; *Feldman et al.*, 2005]. To date, observations of water ice clouds have been necessarily limited to daytime. In particular, cloud opacity retrievals derived from Mars Global Surveyor (MGS) Thermal Emission Spectrometer (TES) spectra have only been performed for the case of a high thermal contrast against a hot surface (>220 K) and so are only available for 2 pm observations [*Smith*, 2004]. Here we describe the mapping of nighttime clouds by identifying their radiative influence on the seasonal evolution of surface brightness temperatures observed by TES. We also show spatial maps of atmospheric absorption derived from Mars Orbiter Laser Altimeter (MOLA) radiometry that provide corroboration of this technique [*Neumann and Wilson*, 2006; *Sun et al.*, 2006]. Finally we compare MGCM simulations with and without radiatively active water ice clouds to show that clouds can have a detectable influence on nighttime surface temperature.

2. Data and Analysis

[3]   Surface temperature is a strong function of the surface thermal inertia and albedo and is also significantly influenced by atmospheric opacity [*Mellon et al.*, 2000]. We have used MGS TES surface temperatures to obtain improved thermal inertia (TI) fields suitable for use in versions of the GFDL MGCM employing spatial resolutions of $5 \times 6°$ and $2 \times 2.4°$. We have binned TES morning (2 am) and afternoon (2 pm) surface brightness temperatures (T_{23} and T_7 respectively) at the GCM spatial scale with 5° resolution in areocentric longitude (L_s). We use the MGCM radiation code to calculate simulated T_7 and T_{23} for direct comparison with the observed temperatures. A best fit thermal inertia field was derived by an iterative process starting with an initial thermal inertia field [*Mellon et al.*, 2000] and using a fixed albedo field [*Christensen et al.*, 2001]. We used the available estimates of dust opacity for fitting observed temperatures during the variably dusty perihelion season [*Wilson and Smith*, 2006]. By construction, the newly fitted TI fields allow the MGCM to accurately predict the observed 2 am and 2 pm temperatures in seasons and locations where our assumptions of atmospheric opacity are well founded. Since opacity leads to an increase in morning temperature and a decrease in afternoon temperature [*Mellon et al.*, 2000], seasonally evolving differences between observed and simulated temperatures largely reflect the influence of dust and/or water ice clouds not accounted for in a given simulation. During the $L_s = 30-150°$ period, dust optical depth is at its annual minimum and has only a minor influence on surface temperatures. This allows the influence of ice clouds in the Northern Hemisphere (NH) summer season to be isolated and spatially mapped.

[4]   The GFDL MGCM simulates the circulation of the Martian atmosphere with a comprehensive set of physical parameterizations [*Wilson and Hamilton*, 1996; *Hinson and Wilson*, 2004]. These include parameterizations for radiative transfer associated with CO_2 gas and aerosols. The dust aerosol may be specified or can be allowed to evolve with the circulation. These formulations yield close agreement between observed (TES) and simulated atmospheric temperatures. The water cycle is represented by surface ice deposition and sublimation, atmospheric transport and ice cloud formation [*Richardson and Wilson*, 2002]. The predicted ice clouds are optionally radiatively active. We use a 2-stream method to account for aerosol scattering and absorption when calculating shortwave and longwave radiative fluxes [*Hinson and Wilson*, 2004]. The relevant optical properties are functions of wavelength, aerosol composition and particle size. Cloud radiative properties in the IR are

[1]Geophysical Fluid Dynamics Laboratory, National Oceanic and Atmospheric Administration, Princeton, New Jersey, USA.
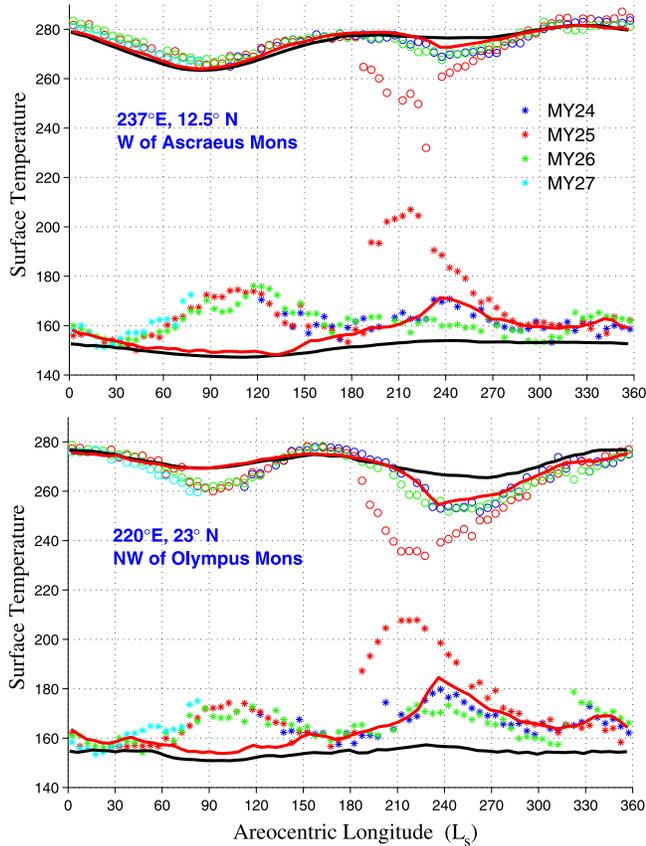[2]NASA Goddard Space Flight Center, Greenbelt, Maryland, USA.

Figure 1. The seasonal variation of 2 am (stars) and 2 pm (circles) TES surface temperatures for two locations in the Tharsis region. Four Mars years are shown: MY24 (blue), MY25 (red), MY26 (green) and MY27 (cyan). The black curves represent the corresponding temperatures from the low dust reference simulation and the red curves show temperatures from a simulation with variable dust opacity.

planet during the relatively clear NH spring/summer season when the low dust opacity assumed in the reference simulation most closely approximates that of the actual atmosphere. Therefore the development of warm nighttime temperature anomalies at the two locations shown in Figure 1 in the solstice season is particularly striking. The evolution of these anomalies is strongly correlated with the waxing and waning of the tropical cloud belt evident in daytime ice opacity retrievals [*Smith*, 2004]. The formation of the cold (−8 K) 2 pm anomaly to the NW of Olympus Mons (Figure 1, bottom) is directly related to the daytime ice opacity associated with a localized orographic cloud (see Figure 2). Note that we have not accounted for water ice cloud opacity, which is not available for nighttime observations. The development of the large amplitude (>20 K) nighttime anomalies in Figure 1 is evidently not associated with albedo or dust influences, but is most readily attributed to enhanced IR emission from nighttime water ice clouds.

[6] Seasonally varying spatial maps of surface temperature anomaly (ΔT) have been constructed by subtracting the simulated reference temperature fields from the corresponding observed temperatures in each spatial cell. The influence of clouds can be isolated by differencing the solstice season anomaly field with an anomaly field for a period when clouds are less prominent. We use the reference simulation at $L_s = 45°$ for this purpose, as ΔT is minimal in this season and the low (dust only) opacity assumption is most realistic, as suggested in Figure 1. Differencing the two anomaly fields minimizes the influence of systematic biases in the best fit thermal inertia field used in the reference simulation.

[7] We now compare the spatial distribution of daytime water ice clouds derived by several independent techniques. Figure 2a shows the spatial distribution of daytime clouds in the Tharsis region as seen in Mars Orbiter Camera (MOC) imagery while Figure 2b shows 12 μm opacity derived from TES IR spectra [*Smith*, 2004]. Figure 2c shows the ratio

described by *Wolff and Clancy* [2003]. The simulated clouds are assumed to have an effective radius of 4 μm appropriate for low-latitude aphelion-season clouds. Our simulations employ 2 × 2.4° spatial resolution.

3. Results

[5] The seasonal variations of observed and simulated 2 am and 2 pm surface temperature for two locations in the Tharsis region are shown in Figure 1. The solid curves show temperatures from a reference simulation with fixed weak dust opacity (visible $\tau = 0.15$) representing relatively clear sky conditions. The red curves show the model response to dust opacity varying according to TES dust retrievals from Mars Years (MY) 24−25 [*Smith*, 2004]. Relative to the reference simulation there are large perturbations in both daytime and nighttime temperatures due to dust storm activity in the perihelion season ($L_s = 180-350°$). The influence of the 2001 global dust storm in MY25 is particularly prominent. Differences between observed and simulated temperatures are typically < 3 K over much of the
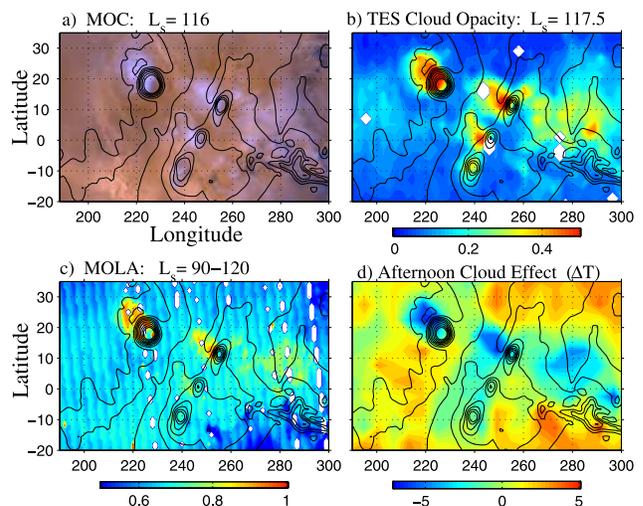

Figure 2. The spatial pattern of daytime (2 pm) clouds in the Tharsis region during NH summer solstice as revealed by (a) MOC imagery, (b) infrared opacity derived from TES spectra, (c) extinction derived from MOLA radiometry, and (d) the daytime surface temperature anomaly, $\Delta T(L_s = 115°) - \Delta T(L_s = 45°)$.
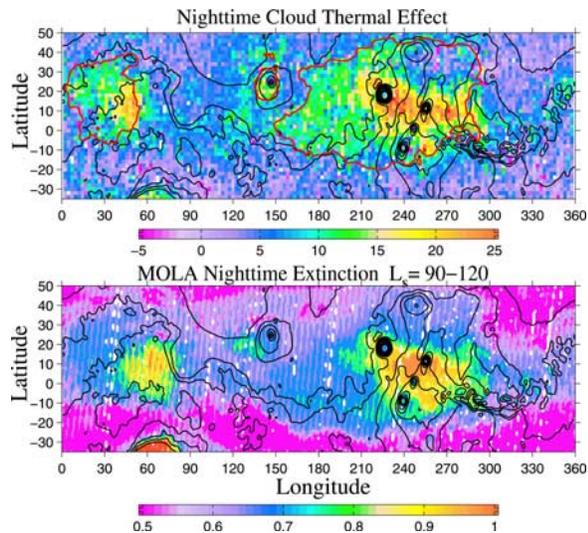
Figure 3. (top) The thermal influence of nighttime clouds indicated by the difference between surface temperature anomaly fields constructed for $L_s = 110–120°$ and $L_s = 40–50°$. Red contours enclose regions of relatively low surface thermal inertia. (bottom) Nighttime MOLA absorption distribution.

between active bidirectional reflectance and surface reflectivity derived from passive radiometry during non-occulted seasons [*Sun et al.*, 2006], which provides a measure of atmospheric extinction at 1 μm. Complete extinction is evident on the NW flank of Olympus Mons and is consistent with $\tau \sim 1.5$. The ratio of visible (1 μm) to 12 μm opacity is roughly unity for clouds with an effective radius of 4 μm. The 2 pm anomaly field, $\Delta T(L_s = 115°) - \Delta T(L_s = 45°)$, is plotted in Figure 2d, which shows the localized cloud cooling effects NW of Olympus Mons and Ascraeus Mons. The four panels provide a consistent description of cloud distribution, suggesting that both MOLA extinction and the daytime temperature anomaly are reliable indicators of thick water ice clouds.

[8] The spatial pattern of the nighttime solstice season temperature anomaly is shown in Figure 3 (top). There is a prominent warm anomaly in the Tharsis region and a weaker and less extensive warm region in Arabia. This pattern is in close agreement with the pattern of strong nighttime extinction revealed by MOLA in Figure 3 (bottom). This agreement strongly supports the interpretation of clouds as being the source of the temperature anomaly. Note that enhanced cloud IR radiation at the surface would be expected to yield a larger temperature influence in regions of low surface thermal inertia, which likely accounts for some of the spatial differences between MOLA extinction and TES ΔT in the Arabia region.

[9] We carried out a MGCM simulation with radiatively active water ice clouds to investigate the plausibility of clouds having the observed temperature effect. The simulated nighttime and daytime cloud opacities are shown in Figures 4 (top) and 4 (middle), respectively for $L_s = 120°$. The daytime opacity field is in reasonable agreement with TES observations [*Smith*, 2004], with a relatively weak tropical cloud belt and an orographic cloud NW of Olympus Mons. The nighttime cloud field is considerably thicker and

more extensive than the daytime cloud field, as has been noted by *Hinson and Wilson* [2004]. Observations have hinted at diurnal cloud variations in the Tharsis region, with a tendency towards decreased opacity away from morning [e.g., *Akabane et al.*, 2002]. *Clancy et al.* [1996] found a solstice season early morning (0630–0900 LT) water ice cloud filling the region between Olympus Mons and the Tharsis ridge, in good qualitative agreement with our results.

[10] Figure 4 (bottom) shows the simulated increase in nighttime surface temperatures relative to the reference simulation which does not include cloud radiative effects. This comparison indicates that enhanced downward infrared radiation from the simulated clouds is able to reasonably account for the observed spatial pattern and amplitude of the surface temperature anomaly shown in Figure 3 (top). This greenhouse influence was anticipated in cloud modeling work by *Colaprete and Toon* [2000]. The simulated cloud opacity of $\sim$1.5 in Figure 4 (top) is consistent with the opacity calculated to account for the peak extinction seen by MOLA [*Neumann and Wilson*, 2006]. Similarly we find that $\tau \sim 1.5$ is sufficient to yield the depression in daytime
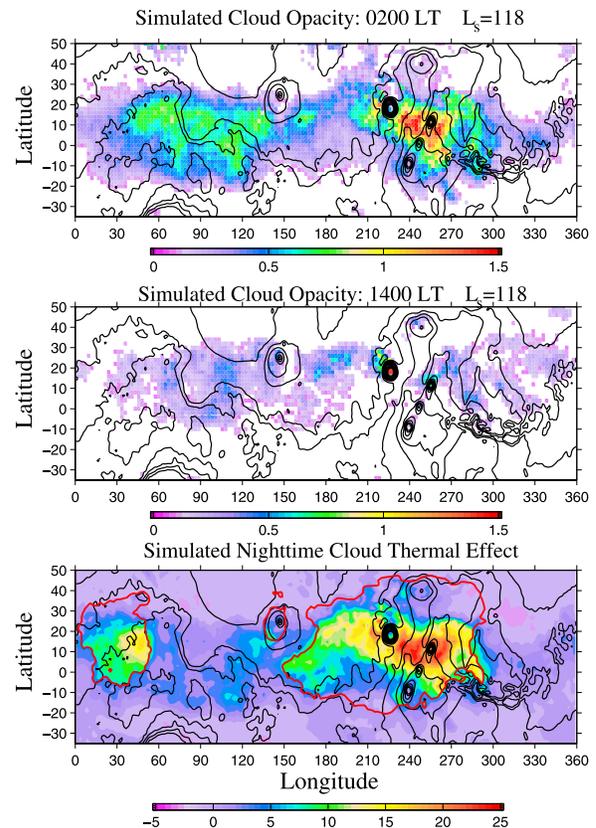

Figure 4. Simulated visible water ice cloud opacity for (top) nighttime and (middle) daytime conditions. (bottom) The simulated surface temperature anomaly is obtained by subtracting the reference surface temperature field from the corresponding surface temperatures from the simulation with radiatively active water ice clouds. As in Figure 3 (top), the red contours enclose regions of low surface thermal inertia.

temperature (T_7) of ~ 8 K seen in Figure 1 (bottom), which is also in agreement with the MOLA analysis.

4. Summary and Discussion

[11] Our indirect cloud retrievals are the first to spatially map the nighttime clouds and provide an estimate of their thermal influence. The close agreement in spatial patterns of MOLA extinction and surface thermal anomaly provides compelling evidence for our interpretation of the surface temperature anomaly. Our MGCM simulations indicate that relatively thick nighttime water ice clouds ($\tau \geq 1$) can provide the enhanced IR radiation at the surface needed to account for the observed temperature anomalies. We conclude from the modeling and MOLA results that the solstice season nighttime cloud distribution is considerably thicker and more extensive than the daytime clouds. Therefore daytime cloud observations provide an incomplete, and possibly misleading, description of Martian cloud activity.

[12] *Hinson and Wilson* [2004] used the same model (but with lower spatial resolution) to show that atmospheric cooling (and heating) by radiatively active water ice clouds can explain the presence of large amplitude, early morning (0400 LT) atmospheric temperature inversions observed in the Tharsis region. We note that the Tharsis clouds described in this study are able to simultaneously account for the observed atmospheric temperature profiles described by *Hinson and Wilson* [2004] and the surface temperature influence described here. We suggest that this consistency provides further support for the radiative influence of ice clouds and highlights the ability of MGCMs to interpret diverse observations as aspects of the same physical process. An examination of the simulation results indicates that the dominant daytime clouds are typically associated with strong circulations localized to volcanoes as described by *Michaels et al.* [2006], while the nighttime clouds reflect circulation influences on a larger scale. In particular, thermal tides modulated by Tharsis-scale variations in topography appear to play a significant role in shaping the diurnal variation and vertical structure of tropical water ice clouds [*Hinson and Wilson*, 2004].

[13] It is anticipated that our mapping of water ice clouds will provide a sensitive constraint for simulations of the atmospheric circulation and water vapor transport. We are currently investigating the role of cloud radiative effects on zonal mean atmospheric temperature at tropical and polar latitudes. Our simulations suggest that radiative cooling by polar hood clouds can influence the structure of the polar vortex during the spring and fall seasons. This can then modify the properties of baroclinic waves embedded in the polar vortex.

References

Akabane, T., T. Nakakushi, K. Iwasaki, and S. M. Larson (2002), Diurnal variation of Martian water-ice clouds in Tharsis region of the low latitude cloud belt: Observations in 1995–1999 apparitions, *Astron. Astrophys.*, *384*(2), 678–688.

Christensen, P. R., et al. (2001), Mars Global Surveyor Thermal Emission Spectrometer experiment: Investigation description and surface science results, *J. Geophys. Res.*, *106*(E10), 23,823–23,872.

Clancy, R. T., et al. (1996), Water vapor saturation at low altitudes around Mars aphelion: A key to Mars climate?, *Icarus*, *122*, 36–62.

Colaprete, A., and O. B. Toon (2000), The radiative effects of Martian water ice clouds on the local atmospheric temperature profile, *Icarus*, *145*, 524–532.

Feldman, W. C., et al. (2005), Topographic control of hydrogen deposits at low latitudes to midlatitudes of Mars, *J. Geophys. Res.*, *110*, E11009, doi:10.1029/2005JE002452.

Hinson, D. P., and R. J. Wilson (2004), Temperature inversions, thermal tides, and water ice clouds in the Martian tropics, *J. Geophys. Res.*, *109*, E01002, doi:10.1029/2003JE002129.

Mellon, M. T., B. M. Jakosky, H. H. Kieffer, and P. R. Christensen (2000), High-resolution thermal inertia mapping from the Mars Global Surveyor Thermal Emission Spectrometer, *Icarus*, *148*, 437–455.

Michaels, T. I., A. Colaprete, and S. C. R. Rafkin (2006), Significant vertical water transport by mountain-induced circulations on Mars, *Geophys. Res. Lett.*, *33*, L16201, doi:10.1029/2006GL026562.

Montmessin, F., F. Forget, P. Rannou, M. Cabane, and R. M. Haberle (2004), Origin and role of water ice clouds in the Martian water cycle as inferred from a general circulation model, *J. Geophys. Res.*, *109*, E10004, doi:10.1029/2004JE002284.

Neumann, G. A., and R. J. Wilson (2006), Night and day: The opacity of clouds measured by the Mars Orbiter Laser Altimeter (MOLA), *Lunar Planet. Sci.*, *XXXVII*, abstract 2330.

Richardson, M. I., and R. J. Wilson (2002), Investigation of the nature and stability of the Martian seasonal water cycle with a general circulation model, *J. Geophys. Res.*, *107*(E5), 5031, doi:10.1029/2001JE001536.

Richardson, M. I., R. J. Wilson, and A. V. Rodin (2002), Water ice clouds in the Martian atmosphere: General circulation model experiments with a simple cloud scheme, *J. Geophys. Res.*, *107*(E9), 5064, doi:10.1029/2001JE001804.

Smith, M. D. (2004), Interannual variability in TES atmospheric observations of Mars during 1999–2003, *Icarus*, *108*, 148–165.

Sun, X., G. A. Neumann, J. B. Abshire, and M. T. Zuber (2006), Mars 1064-nm spectral radiance measurements from the receiver noise response of the Mars Orbiter Laser Altimeter, *Appl. Opt.*, *46*(17), 3960–3971.

Wilson, R. J., and K. P. Hamilton (1996), Comprehensive model simulation of thermal tides in the Martian atmosphere, *J. Atmos. Sci.*, *53*, 1290–1326.

Wilson, R. J., and M. D. Smith (2006), The effects of atmospheric dust on the seasonal variation of Martian surface temperature, paper presented at 2nd International Workshop on Mars Atmosphere Modelling and Observations, Cent. Natl. D'Etud. Spatiales, Granada, Spain, 27 Feb. to 3 Mar.

Wolff, M. J., and R. T. Clancy (2003), Constraints on the size of Martian aerosols from Thermal Emission Spectrometer observations, *J. Geophys. Res.*, *108*(E9), 5097, doi:10.1029/2003JE002057.

———————————
G. A. Neumann, NASA Goddard Space Flight Center, Code 698, B33 Room G207, Greenbelt, MD 20771, USA.

M. D. Smith, NASA Goddard Space Flight Center, Code 693, Greenbelt, MD 20771, USA.

R. J. Wilson, Geophysical Fluid Dynamics Laboratory, NOAA, P.O. Box 308, Princeton, NJ 08542, USA. (john.wilson@noaa.gov)